Available online at www.sciencedirect.com
ScienceDirect
Materials and Design 29 (2008) 305–318
Materials & Design
www.elsevier.com/locate/matdes

Design and analysis of a long fiber thermoplastic composite tailcone for a tank gun training round

Uday K. Vaidya [a,*], Juan C. Serrano [a], Alejandro Villalobos [a], James Sands [b], James Garner [b]

[a] University of Alabama at Birmingham, Department of Materials Science and Engineering, 1150 10th Avenue South (BEC 254), Birmingham, AL 35294, USA
[b] Army Research Laboratory, Aberdeen, Maryland, USA

Received 1 September 2006; accepted 7 February 2007
Available online 2 March 2007

Abstract

The increasing demand for low cost composites in military applications is accompanied by the need to develop cost-effective and high-performance material forms and processing technologies. Innovative composite technologies (material forms, fabrication processes, and design and simulation) have the potential to provide effective solutions for reducing weight and cost of weapon systems and ammunitions. A kinetic energy (KE) penetrator is used as tank ammunition and concentrates an extremely high amount of kinetic energy over a relatively small surface area of the target. In this study, the design and analysis of a tailcone (which is a subcomponent) of an artillery training round (conventionally manufactured of aluminum) using long fiber thermoplastic (LFT) composite material and processing technologies was conducted. The function of a tailcone is to stabilize and limit the range of travels of the projectile. Finite element analysis was used to design and evaluate the response of a LFT composite tailcone to pressure, gravitational load, and temperature during its path from inside the bore of the gun up to its flight in air. Subsequent field testing of the designed composite training round served as a validation of the finite element models developed. By implementing the proposed LFT composite tailcone, a cost savings in the order of 70% is projected in comparison to the existing aluminum design, without compromising performance.

Keywords: A. Polymer matrix composites; B. Thermoplastic composites; C. Extrusion; D. Impact and ballistic

1. Introduction

A kinetic energy (KE) penetrator is an armament used in an artillery tank. The basic KE penetrator features a cartridge case, a primer, a projectile, and the propellant [1,2]. When the primer is ignited, the propellant (which is the explosive charge) generates a hot expanding gas that pushes the projectile out of the case. A sabot confines the projectile to the size of the inner diameter of the canon. Practice ammunition also referred to as a 'training round' is often used for training of military personnel. A typical training round contains a slotted aluminum tailcone (shaped in the form of a frustum of a cone); the tailcone comprises a threaded end which mates to the body of the projectile. The tailcone limits the range of the projectile to a permitted maximum distance of travel, and also provides aerodynamic stability to the projectile. The physical characteristics of a typical training round are shown in Table 1. In a field-environment, the projectile has a finned tail instead of a tailcone; the fins enable a longer flight range.

The existing version of a tailcone utilizes machined aluminum, which is a high strength material typically used in aerospace and defense applications such as aircraft fittings, gears and shaft. The aluminum tailcone is expensive due to its alloy composition and high machining costs; a large number of tailcone parts are used by the Army each year.

* Corresponding author. Tel.: +1 205 934 9199; fax: +1 205 934 8485.
E-mail address: uvaidya@uab.edu (U.K. Vaidya).

0261-3069/$ - see front matter © 2007 Published by Elsevier Ltd.
doi:10.1016/j.matdes.2007.02.010

Table 1
General characteristics of the training round

Projectile length (mm)	532
Projectile weight (kg)	8.17
Muzzle exit velocity (m/s)	1427
Target range (m)	3000

The motivation for this work is to develop and demonstrate alternate cost-effective thermoplastic composite materials and processing technologies that could replace the aluminum tailcone without compromising on its performance.

2. Materials

2.1. Material consideration: homopolymers versus LFT

Materials considered as the replacement of aluminum need to comply with the structural and thermal requirements witnessed during firing. From a structural point of view, a material with very high modulus, but a very low strain to failure, would fail catastrophically without significant deformation, when the ultimate load is attained. A material with large deformation capability, but a very low modulus, would deform excessively and not retain the desired shape. Hence, an optimal compromise between ultimate strength, modulus, and maximum deformation was required for the tailcone application. The thermal properties were also very important in the material selection process, because the tailcone resides inside the bore during firing. It is therefore directly exposed to the flash temperature of the combusting propellant. Material properties such as thermal resistance (HDT), thermal conductivity (TC), and melting point (MP) were considered during the material selection phase. Tailcones are usually stored in warehouses for extended periods of time; therefore, degradation of properties due to environmental conditions was another important consideration. Specific properties related to environmental resistance (for storage conditions) and chemical compatibility of the propellant to the material were also considered.

In the present work long fiber reinforced thermoplastics (LFTs) were considered as a materials choice since this family of composites offers high-volume, high rate processability of parts that possess high strength, damage tolerance, and stiffness. LFTs are discontinuous fiber composites that have fiber lengths between 7 and 25 mm depending on the fiber, the matrix and the type of sizing (if any) [4,5]. LFTs are typically made of a low cost thermoplastic polymer like PP, PA, PE, and polycarbonate (PC). reinforced with glass, carbon or aramid fibers. LFTs exhibit high strength, stiffness, and improved impact properties in contrast to short fiber reinforced thermoplastics because of their high fiber aspect ratio (typically >2000 in the case of E-glass/nylon). In addition they can be produced in high volumes; they can be molded to fill complex geometries, are intrinsically recyclable, and possess capacity for parts integration. A detailed description of the LFT technology can be found elsewhere [4,5].

For the tailcone application 40% W_f LFT glass/nylon was chosen based upon initial analysis of three candidate homopolymers. These are polyamides (PAs) also called nylon, polypropylene (PP), and polyetheretherketone (PEEK). Some of these materials have been successfully implemented in similar applications such as kinetic energy penetrator's finned assemblies and obturators [3]. Table 2 compares the properties of the candidate polymer systems. From this table it can be noted that PP has lower modulus, strength, and temperature capability in comparison to nylon and PEEK. From a thermal and structural point of view, PEEK appears to be a suitable candidate. However, PEEK is an expensive material and requires a processing temperature of approximately 650 °F. Although the modulus of PEEK is 10% higher, and its melting temperature is about twice that of nylon, the price of PEEK is over 20 times higher than that of nylon [6]. Nylon 6/6 has excellent high temperature performance (up to 300 °C), high modulus and is cost-effective when compared to other high end engineering polymers. Previous compatibility studies of nylon with the propellant have shown that it is impervious to chemical attack by the propellant used in this type of ammunition. A combination of cost and adequate performance under the before mentioned service conditions was the rationale for choosing nylon as the candidate for the tailcone material.

Table 2
Material properties of considered thermoplastic composite polymers

Property	Nylon 66	PP	PEEK
Density (kg/m^3)	1460	1210	1610
Ultimate strength (MPa)	221	62	186
Modulus (GPa)	13.8	8.3	15.1
Melting temperature (°C)	299	232	399
Thermal conductivity (W/m K)	0.52	0.35	0.39
Specific heat (J/kg K)	2200	2200	1900
Price ($/kg) [6]	3.3	2.2	72.6

3. Design requirements

Based on the structural and thermal data, the tailcone's path from the stage of firing to travel in the air can be divided into three stages of loading. These are classified as in-bore, transition and out-of-bore stages, respectively. These three stages are briefly discussed below.

3.1. In-bore stage

The tailcone resides completely inside the chamber at the moment of firing, and therefore witnesses very high thermal and structural loads. The in-bore pressure and acceleration data versus time for a typical projectile is plotted in Fig. 1 [1]. The projectile takes 6.15 ms to reach the end of the bore, and in that time, the component has to withstand a maximum acceleration of 434,140 m/s^2 (44,300 earth gravities) and a maximum hydrostatic pressure of 406 MPa at 1.95 ms. The tailcone is simultaneously subjected to an average temperature of 1970 K (Fig. 2). While this service temperature is very high in comparison to the reported data [6,7] for the selected materials, the duration of the thermal loading is transient (<6 ms) and

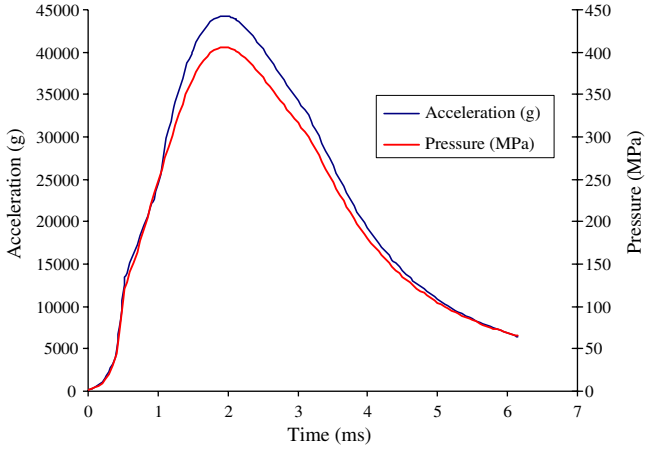

Fig. 1. Acceleration and pressure in-bore for the projectile.

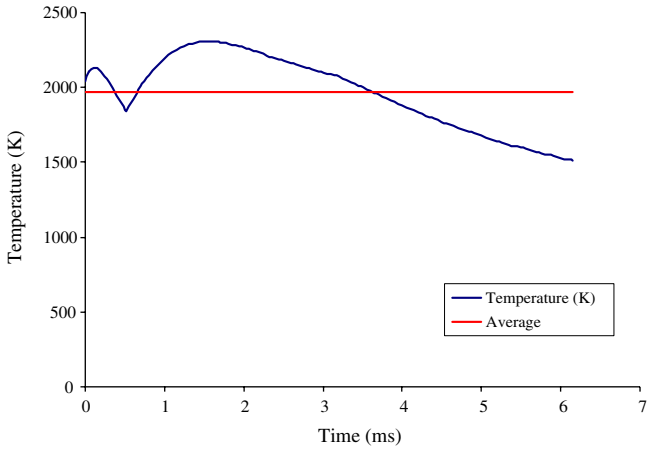

Fig. 2. Temperature in-bore for the projectile.

the LFT composite material does not reach thermal equilibrium due to its inherently low thermal conductivity. Therefore, the effect of temperature on the part is expected to be minimal.

3.2. Transition stage

The most critical stage in terms of stresses witnessed by the tailcone is the transition stage, i.e. when the projectile is on the verge of exiting the barrel. In this stage, the applied pressure is about seven times smaller than the highest pressure the tailcone has to withstand (in-bore), but unlike in the in-bore stage there is a pressure differential of 100 MPa during exit at the muzzle.

3.3. Out-of-bore stage

Aerodynamic forces and frictional heating (around 550 K for 5 s) are witnessed by the tailcone in the out-of-bore stage. Here the applied loads cause stresses in the tailcone that are various orders of magnitude lower than those induced in-bore and in the transition stage. For the out-of-bore stage, the analysis was focused mainly on the temperature rather than on the loads.

4. LFT composite tailcone design

4.1. LFT tailcone design

Two versions of the design and analysis of the LFT composite tailcone are presented. These are referred to as (a) hollow-back (Fig. 3a) and (b) filled-back (Fig. 3b) geometry throughout this manuscript. The hollow-back geometry mimics the external geometry of the presently used aluminum tailcone, while the filled-back geometry was considered since a hollow-back LFT tailcone required design modifications based upon firing trials conducted on them. The design of the tailcone featured a LFT glass/nylon molded composite which houses a molded-in threaded steel insert. The steel insert was considered since (a) it could be machined from bar stock along with the number and type of threads that mate the tailcone to the body of the projectile, and (b) the steel would increase the overall weight of the tailcone to compensate for the low density of the composite; minimizing any variations of the projectile's aerodynamic characteristics. Weight reduction was not a goal for this application because the center of gravity (CG) of the projectile was to remain unchanged with respect to the baseline aluminum design [3].

The harsh conditions during firing and/or flight are difficult to replicate in a lab scale test, and there are no closed form solutions for determining the stresses developed during firing. Finite element analysis (FEA) was used to estimate the stress state, deflection and survivability of the tailcone for the various stages of travel of the projectile (*in-bore*, *transition* and *out-of-bore transition stages*), respectively.

4.2. Finite element mesh details

All structural and thermal simulations were performed using ANSYS 8.0. A two-dimensional (2D) axisymmetric mesh of the tailcone was generated to optimize computational time. This approach assumes that the tailcone is always subjected to the same loading condition regardless of the position around the vertical axis (axisymmetric

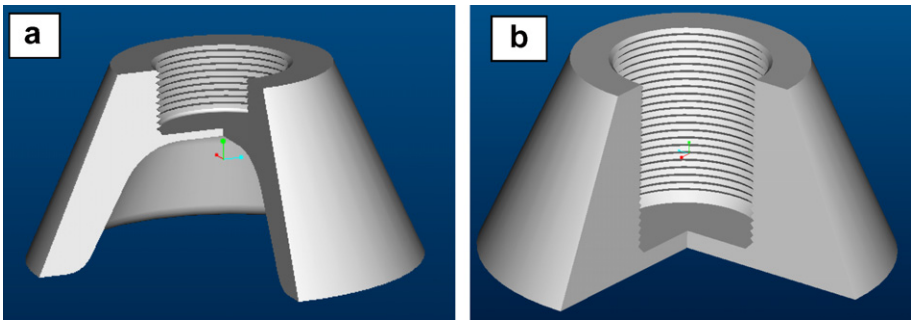

Fig. 3. (a) Hollow-back and (b) back filled tailcone concepts. Note internal cavity for metallic insert.

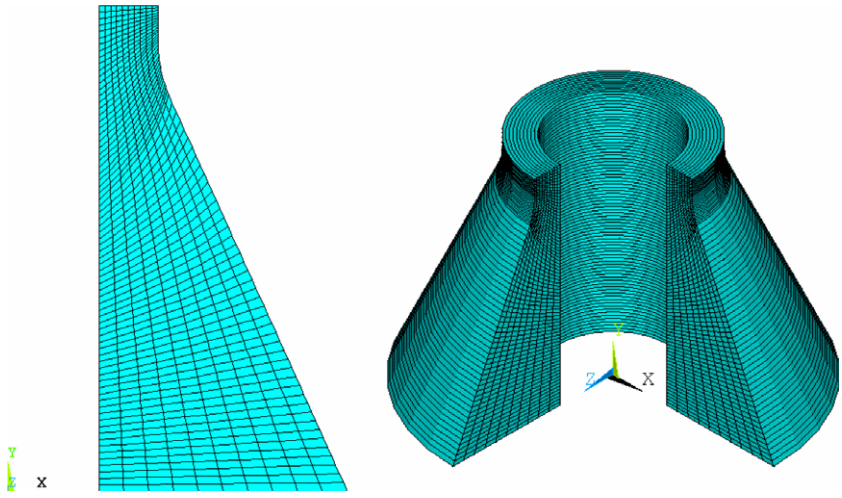

Fig. 4. Finite element mesh for filled-back tailcone generated using quadrilateral elements and corresponding axisymmetric expansion of 2D model.

loading in the tailcone faces). The use of an expandable 2D model allows for the use of a highly refined finite element mesh.

PLANE 42 was used as the element type for the pressure and gravitational simulations. PLANE 42 is commonly used for 2D structural modeling of solid structures. It has capabilities to be used either as a plane element (plane stress or plane strain) or as an axisymmetric element. The element is defined by four nodes having two degrees of freedom at each node; translations in the nodal x and y directions. The element has plasticity, creep, swelling, stress stiffening, large deflection, and large strain capabilities. PLANE 42 only accepts axisymmetric loading. The element input data include four nodes and orthotropic material properties. The default element coordinate system is along global directions. Pressure may be input as surface loads on the element faces.

PLANE 55 was used for thermal analysis of the tailcone both in-bore and out-of-bore. PLANE 55 can be used as a plane element or as an axisymmetric ring element with a 2D thermal conduction capability. The element has four nodes with a single degree of freedom, temperature, at each node. The element is applicable to a 2D, steady-state or transient thermal analysis. The element can also compensate for mass transport heat flow from a constant velocity field. PLANE 55 only accepts axisymmetric loading.

The use of triangular elements is not recommended for bending scenarios (such as the transition stage) due to possible over stiffening of the structure. Therefore, the mesh was generated using the four (4) node quadrilateral option. The mesh generated was based on the outer geometry of the tailcone. The mesh was refined using the smart sizing option. The finite element mesh was checked for individual element connectivity and for other general mesh quality requirements, such as aspect ratio and internal angles. An example of a typical mesh used in this study and its corresponding 3D axisymmetric expansion is shown in Fig. 4 [9].

4.3. Baseline model (aluminum tailcone)

The baseline 7075 aluminum tailcone was simulated under the different loading considerations using FEA. The corresponding material properties for the aluminum alloy 7075 T6 are shown in Table 3. The thermal analysis, i.e. the temperature rise in the in-bore stage and structural analysis, was based upon the pressure and the acceleration exerted on the tailcone.

4.3.1. Thermal analysis of baseline aluminum tailcone: in-bore stage

The initial conditions used in the transient thermal analysis of the aluminum tailcone are shown in Fig. 5. A surface temperature of 1980 K was applied for a time period of 6 ms. The tailcone had an initial temperature of 300 K, which increased as the temperature conducted inward from the outer surface. For the thermal environment, the analysis was conducted taking into account not only the tailcone but also the surrounding component (such as the body of the steel projectile).

The resulting thermal distribution for a 6 ms transient analysis is shown in Fig. 6. While in the steel, the region affected by a temperature higher than 600 °C (873 K) is 0.6 mm deep from the surface, in the aluminum it is 0.8 mm. Aluminum has a high thermal conductivity (167 W/m K), the amount of material lost by thermal effects during firing is seen to be 0.8 mm. However, in order

Table 3
Mechanical properties for 7075 T-6 aluminum and A36 steel

Property	Aluminum	Steel
Density (kg/m^3)	2810	7800
Tensile strength (MPa)	503	350
Modulus (GPa)	71.7	200
Poisson's ratio	0.33	0.29
Thermal conductivity (W/m K)	130	50
Specific heat (J/kg K)	960	500

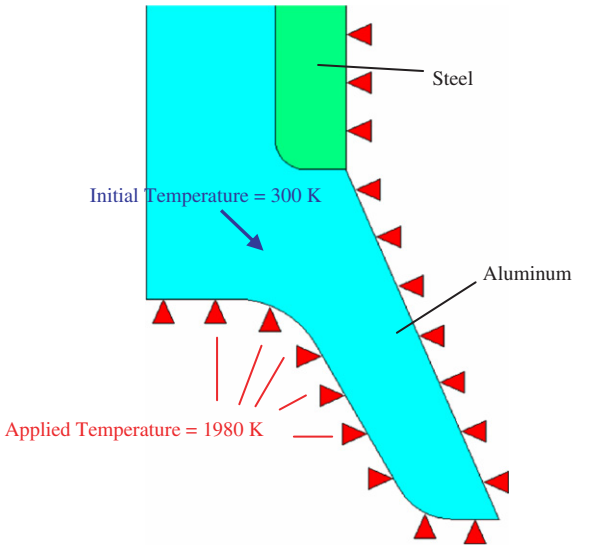

Fig. 5. Initial stages for the in-bore thermal analysis of the aluminum tailcone.

to be conservative, a nominal 1 mm was eliminated from the periphery of all the geometries for the structural analysis that followed.

4.3.2. Thermal analysis of baseline aluminum tailcone: out-of-bore stage

The high speed at which the projectile moves causes friction with air. From previous work [3] it has been shown that the temperature of the airborne projectile can reach approximately 550 K. One of the requirements for the projectile tailcone is that it must survive 5 s (a distance of approximately 8000 m), in flight.

The temperatures resulting from the in-bore analysis were set as the initial conditions for the out-of-bore analysis. Since friction only causes heating in the windward faces of the tailcone, the temperature was not applied to all the faces of the tailcone, but only to the surfaces that are in direct contact with the high speed air flow.

Typical temperature profiles at the end of 5 s into the flight are shown in Fig. 7. The figure shows the rapid increase in temperature in the aluminum tailcone in contrast to the lower heating profile of the steel projectile. This may be attributed to the difference in thermal conductivities of aluminum and steel, respectively.

4.3.3. Structural analysis of baseline aluminum tailcone: general considerations

For the structural analysis, von Mises stresses were evaluated. The von Mises criterion was considered adequate, since the tailcone is made from aluminum, a ductile material [8]. Failure is assumed wherever the resulting von Mises stresses are greater than the yield stress for the material. The safety factor, as used in this study, is defined by

$$n = \frac{\sigma_{\text{von Mises}}}{\sigma_{\text{yield}}} \tag{1}$$

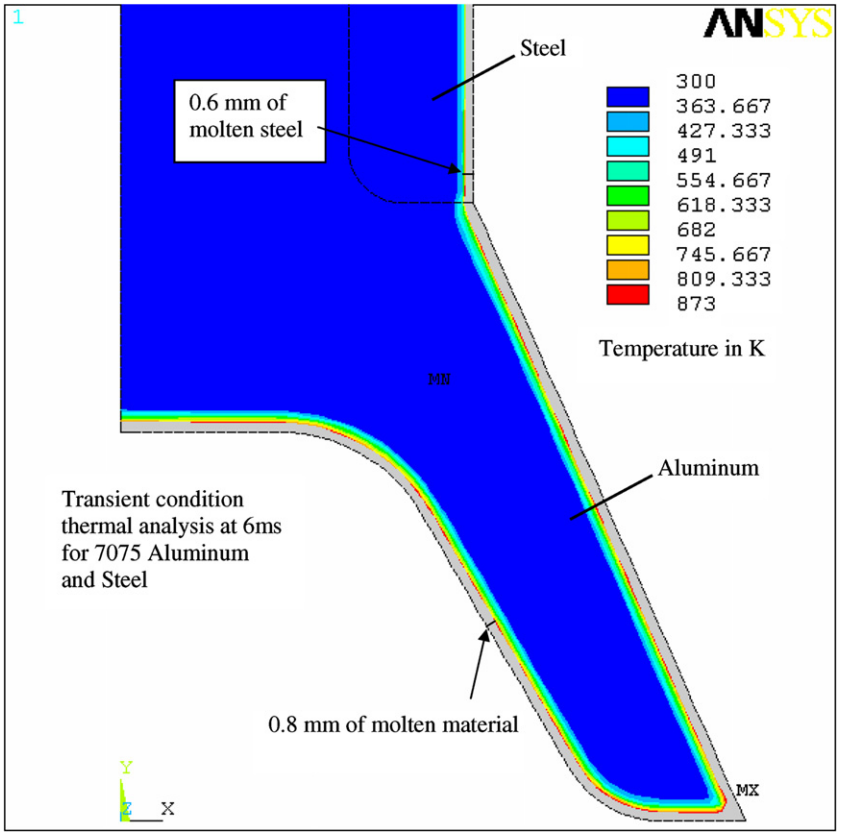

Fig. 6. Transient thermal in-bore analysis for the steel and the aluminum parts. The 0.8 mm of temperature affected molten material is shown.

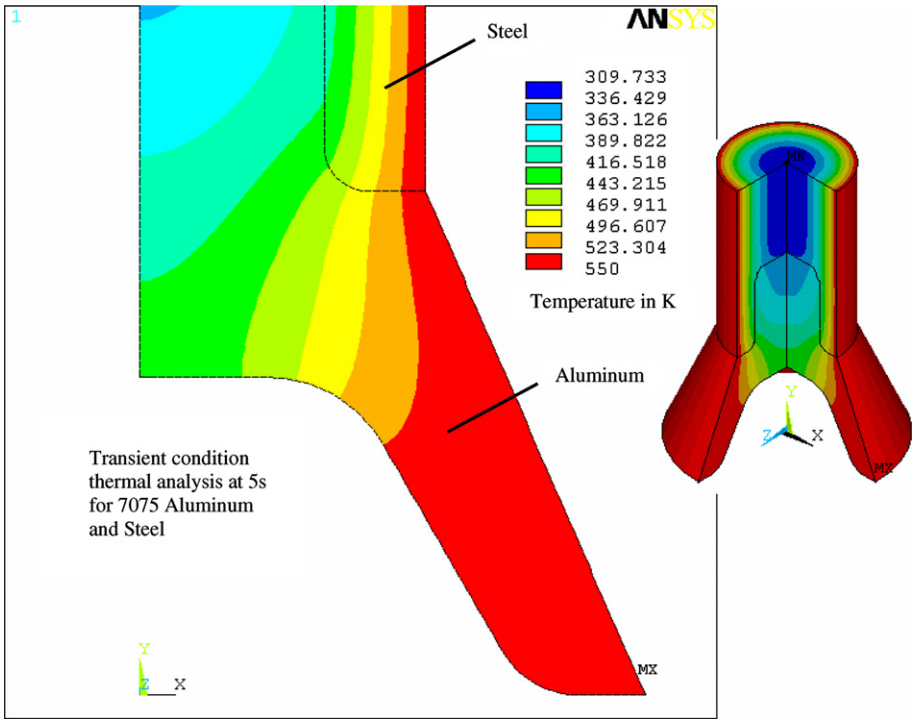

Fig. 7. Transient thermal distribution during out-of-bore stage for the steel projectile and aluminum tailcone. The 3D expansion of the temperature distribution is presented to provide a better understanding of the material response.

where n is the safety factor, $\sigma_{\text{von Mises}}$ the von Mises stress, and σ_{yield} the yield stress for the material.

For the safety factor plots, any region exhibiting a value higher than 1 is considered to have reached failure.

4.3.4. Structural analysis of baseline aluminum tailcone: in-bore stage

The in-bore boundary conditions for the aluminum tailcone are illustrated in Fig. 8a. The constrained elements (displacement in the X and Y directions), applied pressure (405.5 MPa) and inertial acceleration loading (434,061 m/s^2) on the tailcone are shown in the figure. The pressure is a result of the expansion of the propellant during combustion, and the acceleration is the result of change of velocity as the projectile moves inside the muzzle and onto the target.

A static (steady state) analysis on the geometry (it is assumed that the material is not strain rate dependant) was performed, the resulting stresses were obtained, and are plotted in Fig. 8b. From this plot, all stresses are observed to be less than the yield stress of the material. The maximum stress is 321 MPa, which is less than 503 MPa, the yield stress. The region of maximum stress is at the top right corner of the tailcone. The applied constraints in this region are the main cause for this stress concentration. The constraints simulate the reaction of the steel projectile on the loaded tailcone. The steel projectile

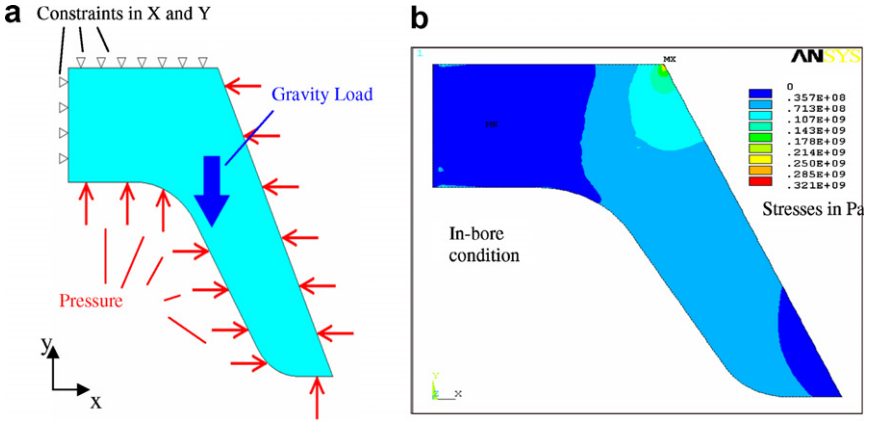

Fig. 8. (a) Boundary conditions for the in-bore structural analysis of the aluminum tailcone and resulting stresses and (b) von Mises stress plot.

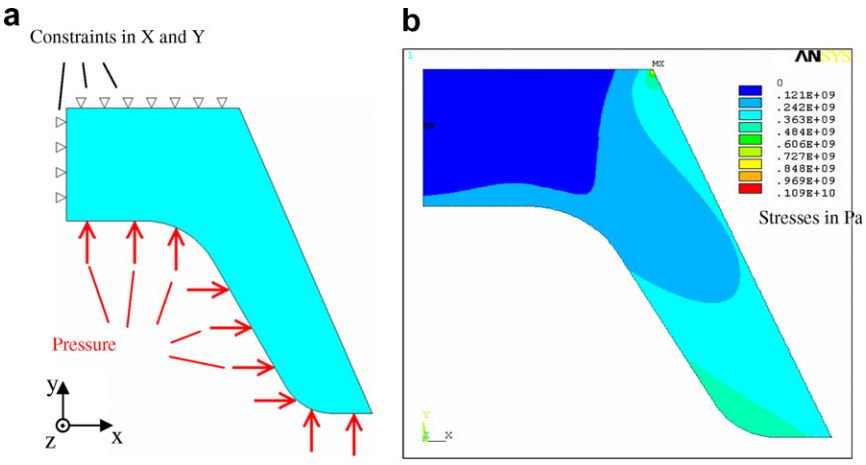

Fig. 9. (a) Boundary conditions for transition regime structural analysis of aluminum tailcone and (b) von Mises stress plot for the aluminum tailcone at transition stage. The maximum stress developed is 1090 MPa and it is observed in the top right corner of the tailcone.

impedes the deformation of the tailcone in the $+y$ direction.

4.3.5. Structural analysis of baseline aluminum tailcone: transition stage

The initial conditions for the transition stage are shown in Fig. 9a. In this case, the applied pressure is 65 MPa (compared to 405.8 MPa for the in-bore initial stages) because pressure is reduced due to escaping gases. The pressure of 65 MPa is only applied to the bottom surface of the tailcone because that is the only surface that witnesses this pressure. The acceleration loading was not considered since the acceleration acts in the opposite direction of the pressure differential, and thereby reduces the stresses developed. The 'no-acceleration' simulation was adopted since it represents a worst case scenario in the transition regime. The results of this analysis are shown in Fig. 9b. The maximum stress is 1090 MPa, which is much higher than the yield strength of the material, but the area affected by this state of stress is very small. There are no other observable regions that could create additional failure paths. The failure region is highly localized. This observed state of stress suggested that the transition stage is much more severe than the in-bore stage.

4.4. Hollow-back LFT composite tailcone

As done with baseline aluminum, thermal analysis was also performed for the 40% W_f E-glass/nylon LFT tailcone for the in-bore and out-of-bore stages, respectively. The boundary stages were the same as applied to the baseline aluminum model. A schematic of the boundary conditions illustrating the LFT tailcone, the aluminum insert and the body of the projectile is shown in Fig. 10a.

4.4.1. Thermal analysis for LFT hollow-back tailcone: in-bore stage

The results for the transient in-bore thermal simulation for the LFT hollow-back tailcone are shown in Fig. 10b. From the thermal distribution, it can be observed that although the maximum used temperature for the LFT material is lower than for that used for aluminum, the

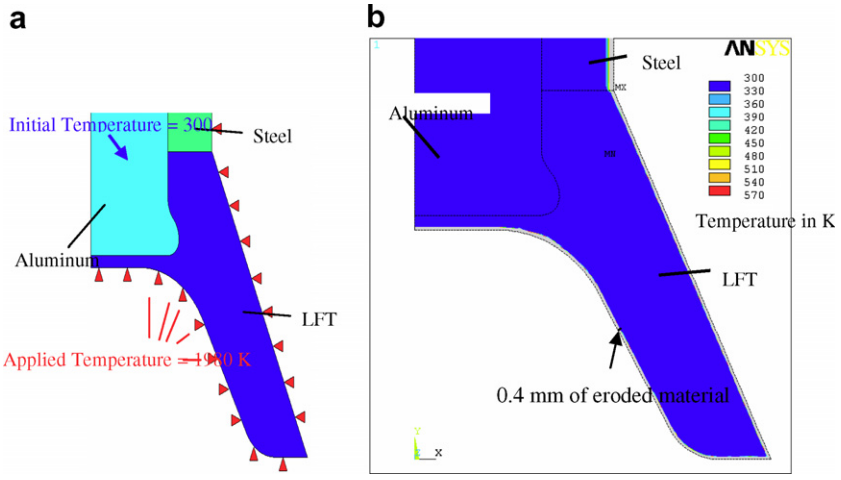

Fig. 10. (a) Boundary conditions for in-bore thermal analysis of hollow-back LFT tailcone and (b) resulting thermal distribution. Note small heat affected region for LFT tailcone in comparison to aluminum design.

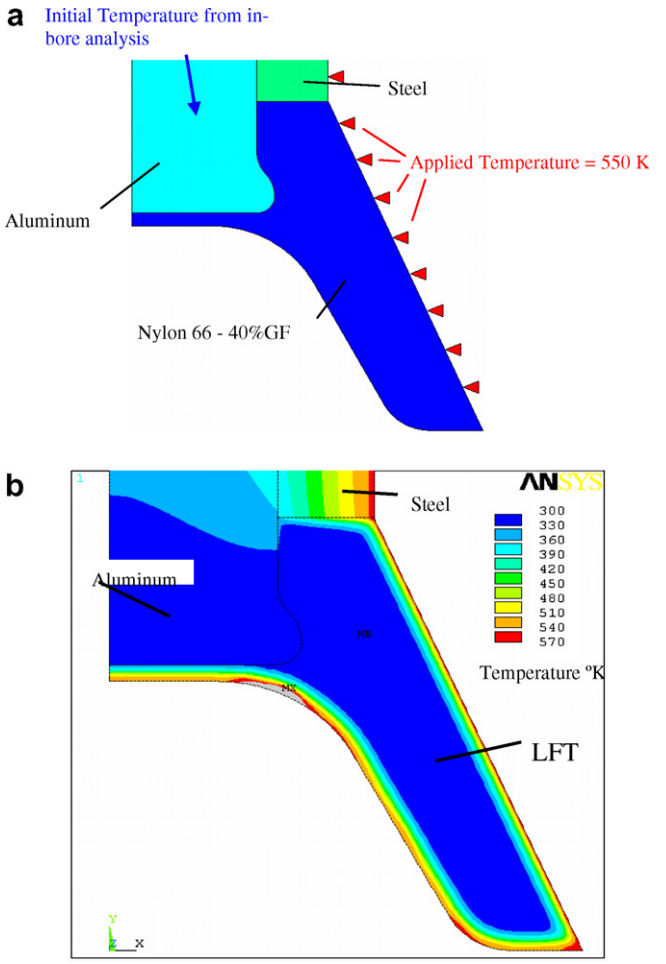

Fig. 11. (a) Boundary conditions for out-of-bore regime thermal simulation on hollow-back LFT tailcone and (b) resulting thermal distribution on LFT tailcone.

lower thermal conductivity of the LFT (0.5 W/m K) reduces the heat affected zone in comparison to the aluminum (167 W/m K) design by 50%. The amount of LFT material that would degrade by thermal effects during firing is seen to be only 0.8 mm.

4.4.2. Thermal analysis for LFT hollow-back tailcone: out-of-bore stage

The in-bore stage results were used as input for the out-of-bore stage thermal analysis. Identical boundary conditions as in the baseline aluminum case were applied. The applied boundary conditions are shown in Fig. 11a, and the results of this simulation are shown in Fig. 11b. The highest temperature observed at the 5 s time interval is 570 K which corresponds to the melting point of the LFT material. A temperature concentration region is located in the inner shoulder of the tailcone due to the residual heating from the in-bore stage.

4.4.3. Structural analysis of LFT hollow-back tailcone: general overview

Fiber fracture, matrix failure, interfacial failures and buckling are typical failure mechanisms in composite materials. For the LFT tailcone more than one failure mechanism may be involved. For the structural analysis of the composite tailcone, the Tsai–Wu failure criterion was adopted, since this criterion evaluates the survival of the composite in an overall sense [10]. The Tsai–Wu criterion has been developed for anisotropic materials (laminated composites). In the case of the LFT tailcone, the properties are not directionally tailored like in a laminated composite. However, there is anisotropy due to preferential fiber distribution, inherent to the compression molding of the LFT material. The properties also vary when the LFT

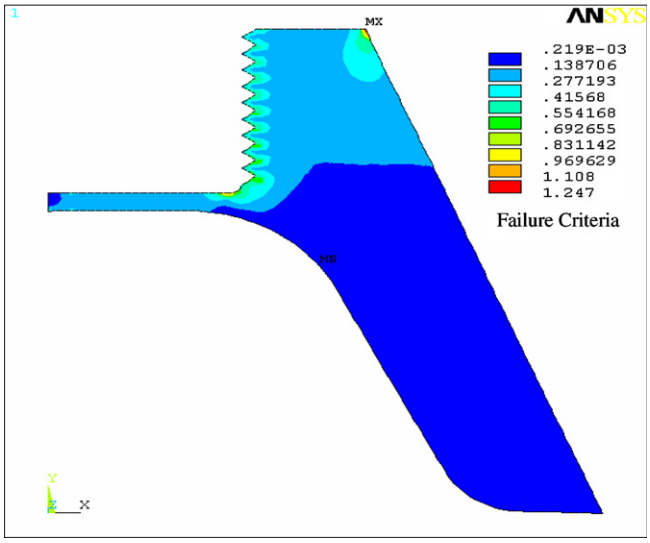

Fig. 12. Tsai–Wu failure criteria plot for hollow-back LFT tailcone subjected to in-bore stages. The maximum value is 1 and it is located at top right part of the tailcone due to the presence of the steel projectile in the top right corner of the tailcone. Note stress concentration at threads.

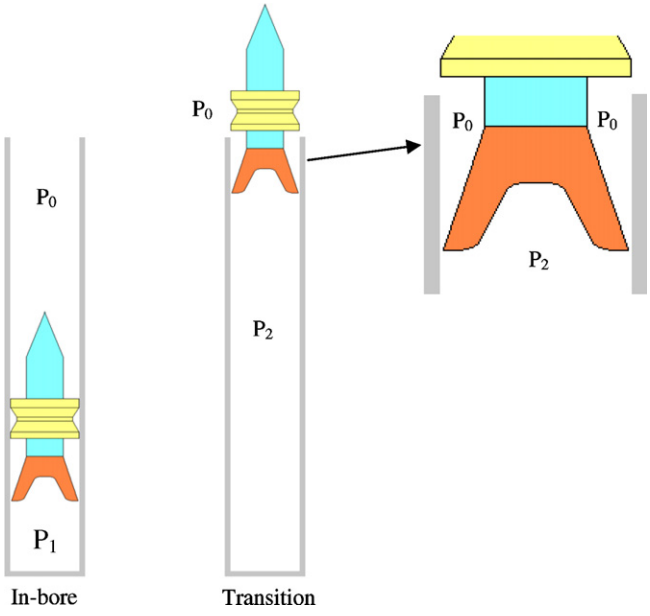

Fig. 13. In-bore and transition stages for analysis of the tailcone.

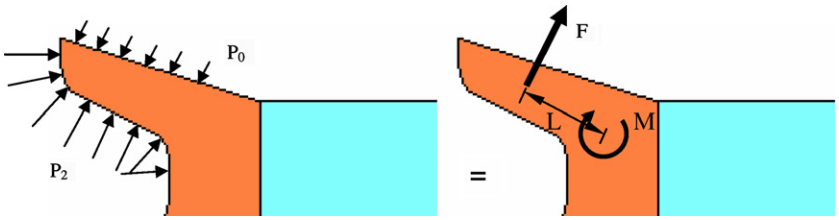

Fig. 14. Transformation of applied pressure into a force and a moment. Note that $P_2 \gg P_0$.

material is loaded under tension or under compression. For example, a 15% improvement was found in the compressive strength in comparison with the tensile strength for nylon 66 with 40% W_f glass fiber [7]. Hence, the use of the Tsai–Wu criterion was deemed appropriate in the present work.

The failure criterion used by ANSYS is a 3D version of the Tsai–Hill 2D criteria.

ANSYS uses the strength ratio as a form of Tsai–Wu failure criterion in a 3D version of the Tsai–Hill 2D criterion given by

$$\xi_2 = \frac{1}{-\frac{B}{2A} + \sqrt{\left(\frac{B}{2A}\right)^2 + \frac{1}{A}}} \tag{2}$$

where

$$A = -F_{xx}\sigma_x^2 - F_{yy}\sigma_y^2 - F_{zz}\sigma_z^2 + \frac{\sigma_{xy}^2}{S_{xy}^2} + \frac{\sigma_{yz}^2}{S_{yz}^2} + \frac{\sigma_{xz}^2}{S_{xz}^2} - \sqrt{F_{xx}F_{yy}}\sigma_x\sigma_y - \sqrt{F_{xx}F_{zz}}\sigma_x\sigma_x - \sqrt{F_{xx}F_{yy}}\sigma_x\sigma_y \tag{3}$$

and

$$B = \left(\frac{1}{X_t} + \frac{1}{X_c}\right)\sigma_x + \left(\frac{1}{Y_t} + \frac{1}{Y_c}\right)\sigma_y + \left(\frac{1}{Z_t} + \frac{1}{Z_c}\right)\sigma_z \tag{4}$$

where σ_x, σ_y and σ_z are the applied stresses in x, y and z; X_t, Y_t and Z_t are the tensile strengths in x, y and z; X_c, Y_c and Z_c are the compressive strengths in x, y and z; S_{xy}, S_{xz} and S_{yz} are the shear strengths in the xy, xz and yz planes; F_{xx}, F_{yy} and F_{zz} are the strength ratio terms from [11]; and ξ_2 is the value of Tsai–Wu strength ratio.

For the structural simulations, the contact zone between the tailcone and the aluminum insert was modeled including the detail of the insert threads.

4.4.4. Structural simulation of hollow-back LFT tailcone: in-bore stage

The boundary conditions were applied as equivalent to the baseline aluminum model. The resulting failure criteria plot can be observed in Fig. 12. The stresses developed resulted in a maximum Tsai–Wu ratio of 1.2, which is 24.7% higher than the allowable limit for the glass/nylon LFT. The highest stress occurs at the top right corner because of the steel projectile that impedes the displacement of the LFT tailcone. Small areas of stress concentrations can be observed in the individual threads as a result of the applied loads.

4.4.5. Structural simulation of hollow-back LFT tailcone: transition stage

The boundary conditions were equivalent to those applied for the baseline aluminum design simulating the transition stage. The constraints were carefully applied to replicate the bending moment which results from the pressure differential occurring during the transition stage (Fig. 13). In order to simulate the conditions at the transition stage, a pressure differential of 100 MPa was applied between the two exposed surfaces of the tailcone (i.e. $P_0 = 100$ kPa, $P_2 = 100.1$ MPa) as illustrated in Fig. 14. It is in this stage where the high pressure built up inside the muzzle is reduced to the atmospheric pressure of the surroundings. It was foreseen that the pressure differential would cause a bending moment on the tailcone as shown in Fig. 14.

The results for the Tsai–Wu failure criteria are shown in Fig. 15. The resulting state of stresses shows failure as evident from the Tsai–Wu ratio of 3.7. A failure path which grows from the lowest thread in the insert and propagates to the upper right corner of the tailcone can be identified. Anything below the dashed line depicted in Fig. 15 is expected to fail as a result of the bending moment applied.

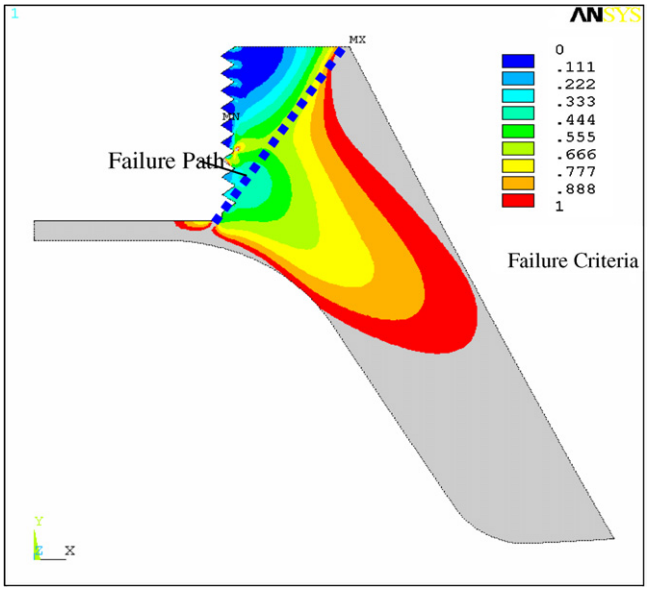

Fig. 15. Details of the Tsai–Wu failure criteria plot for the hollow-back LFT tailcone at the transition regime. Note the failure path created between the lowest thread of the insert and the upper right corner of the tailcone.

4.4.6. Field tests for the hollow-back LFT tailcone

The testing of the LFT tailcone(s) mounted to the training round was conducted at Aberdeen Proving Grounds (APG), Maryland. The testing was carried out to verify the predictions from the simulations using high-speed photography. The projectiles were photographed during flight at a distance of 15 m from the exit of the barrel (Fig. 16). The tailcone is seen to have failed after exiting from the bore. By comparing the images with the predicted failure path of the finite element model (Fig. 15), it may be noted that the model accurately represents the failure of the tailcone at the transition stage. The tailcone design was hence modified, as discussed in the section that follows.

4.5. Filled-back LFT tailcone

From results of the hollow-back LFT tailcone testing, it was deduced that the transition stage caused failure of the glass/PP LFT tailcone. The hollow-back design was initially adopted to mimic the existing 7075 aluminum tailcone, and to minimize material usage to reduce cost to the extent possible. The hollow-back tailcone design was reevaluated and an LFT material filled-back tailcone concept was developed. In the filled-back geometry, the basic

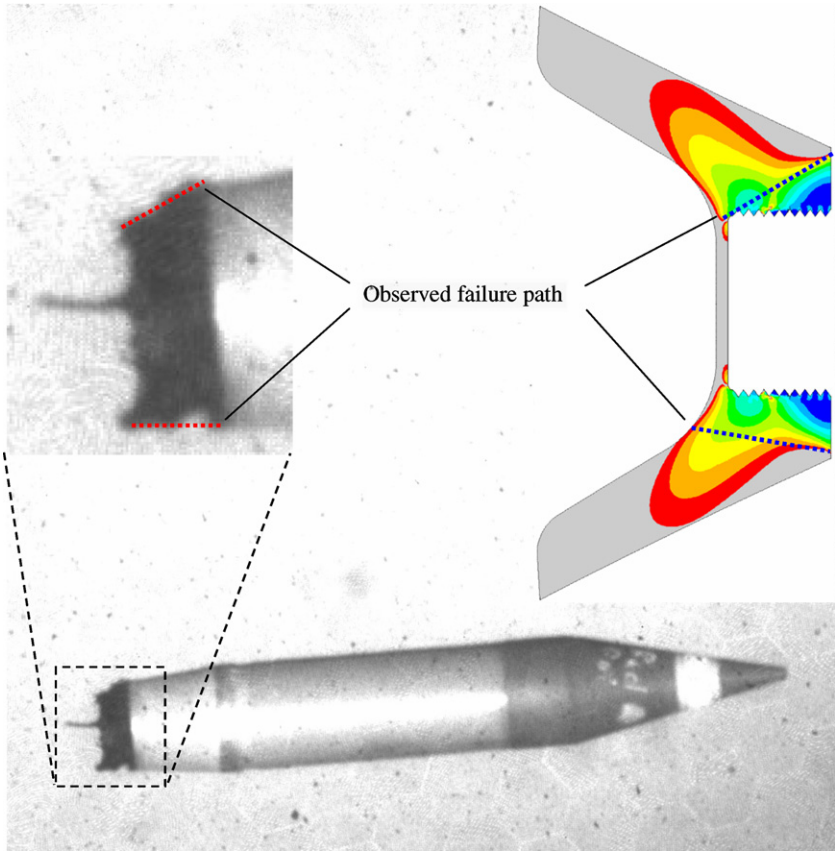

Fig. 16. Field test of hollow-back LFT tailcone mounted projectile 15 m away from barrel exit. The failure path coincides with the FEA analysis.

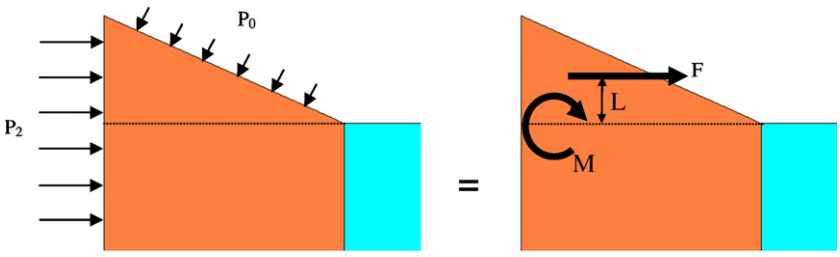

Fig. 17. Transformation of the applied pressures into a force and a moment for the filled-back LFT tailcone concept. Note smaller resulting bending moment at the transition regime.

approach was to create a tailcone which would accomplish the same functions as the aluminum tailcone, such as providing stability, alignment and drag for deceleration. The bending moment imparted at the transition stage would be minimized in the redesigned tailcone. This bending moment was the primary cause of failure of the hollow-back tailcone. Fig. 17 illustrates the filled-back tailcone concept, and the reduced bending moment on the tailcone at the transition stage. The magnitude of the applied pressure behind the tailcone, P_2, is the same as in the hollow-back geometry. The difference, however, lies in the location where the pressure is applied. In the case of the hollow-back tailcone this area was 26,500 mm^2, while in the filled-back tailcone this area is only 10,900 mm^2, which is 41% of the original area. With a smaller area, the force is also smaller, i.e. 41% of the original force.

As with the hollow-back tailcone, a molded-in metal threaded insert was used to connect the tailcone to the main body of the projectile. The total length of the threaded insert considered was 100 mm. A small layer of polymer on the back of the tailcone (~2 mm) was molded over the insert to seal the insert from the hot expanding gases created during firing, and therefore avoid separation of the tailcone and the insert. The 100 mm insert provided large contact area for the insert and the LFT molded tailcone.

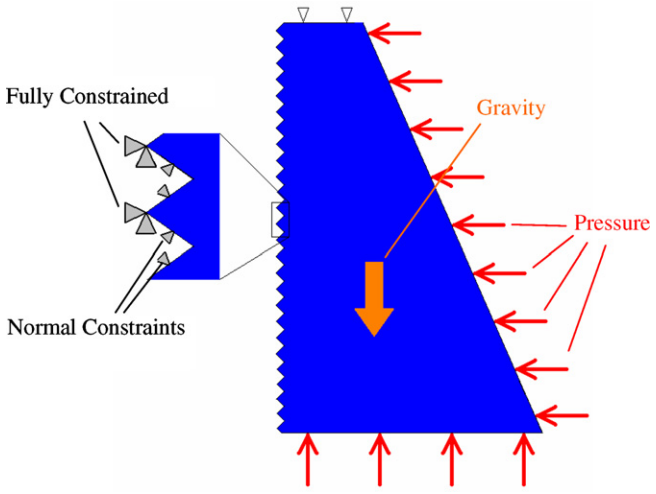

Fig. 18. Boundary conditions for the in-bore structural analysis of the filled-back LFT tail cone. The detail shows the threads as fully constrained at each peak of the threads and normally constrained at each mid-node.

4.5.1. Structural analysis of filled-back LFT tailcone: general overview

The properties of the LFT material of the filled-back tailcone and the metal insert were similar to those used for the hollow-back tailcone. The element types and the design criteria were also the same as for the hollow-back tailcone.

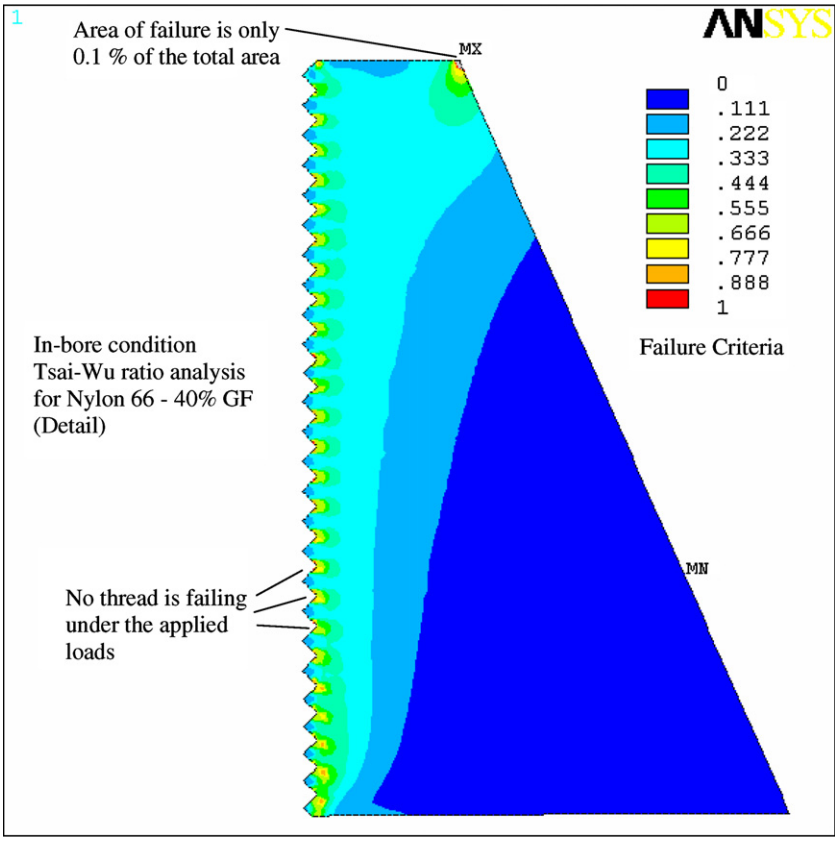

Fig. 19. Tsai–Wu failure criteria plot for the filled-back LFT section of the tailcone at in-bore stages. The maximum value is 1.494 and it is located at the top corner where the LFT meets the steel projectile.

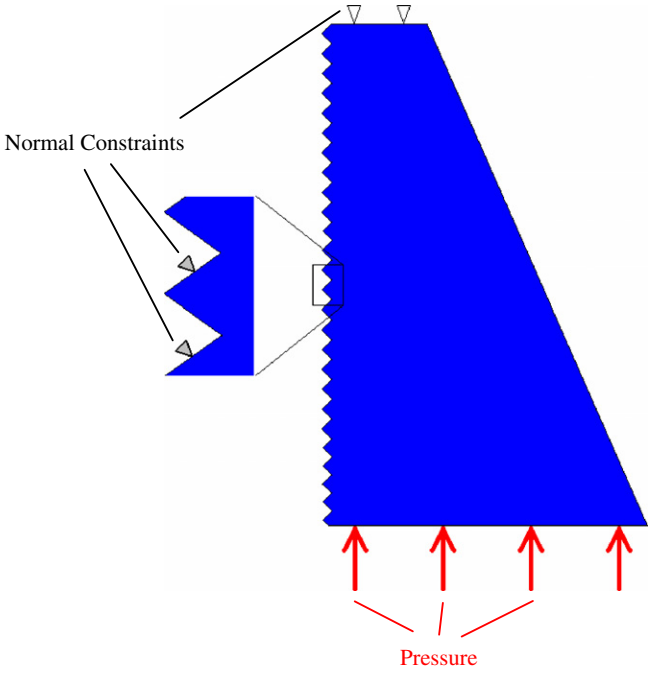

Fig. 20. Boundary conditions for the transition region on filled-back LFT tailcone and 100 mm metallic insert. The detail shows the threads constrained normally in the top surface of each one.

4.5.2. Structural analysis of filled-back LFT tailcone: in-bore stage

The boundary conditions applied to the filled-back LFT tailcone are shown in Fig. 18. In this case, the LFT-to-aluminum interface was treated as an unbounded frictionless interface. The results from this analysis are plotted in Fig. 19. The maximum value of the Tsai–Wu failure criterion is found to be close to 1. However, as with the aluminum baseline, the local failure region is very small. Since this area is resin rich, the nylon is expected to yield locally without propagating the damage into macro cracks. The higher value of the Tsai–Wu failure criterion is not witnessed in the threads, but in the top right corner where the LFT-to-steel interface becomes the stress raiser.

4.5.3. Structural analysis of filled-back LFT tailcone: transition stage

In the case of the hollow-back LFT tailcone, the transition stage was found to be the most critical, and failure was found to be linked to the stresses developed during this stage. The filled-back tailcone was analyzed using equivalent loading and boundary conditions. The applied loads for the filled-back geometry are shown in Fig. 20. The results from the Tsai–Wu analysis for the filled-back geom-

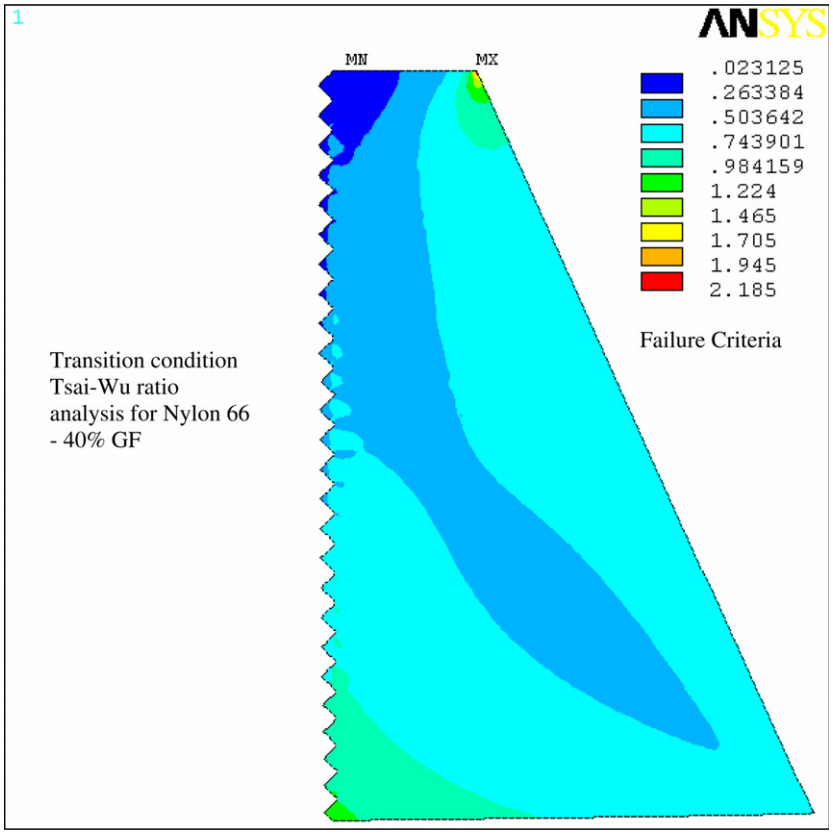

Fig. 21. Tsai–Wu failure criteria plot for the filled-back LFT tailcone at the transition stage. The maximum failure criteria value is 2.185. Failure region is highly localized and does not seem to compromise the integrity of the tailcone.

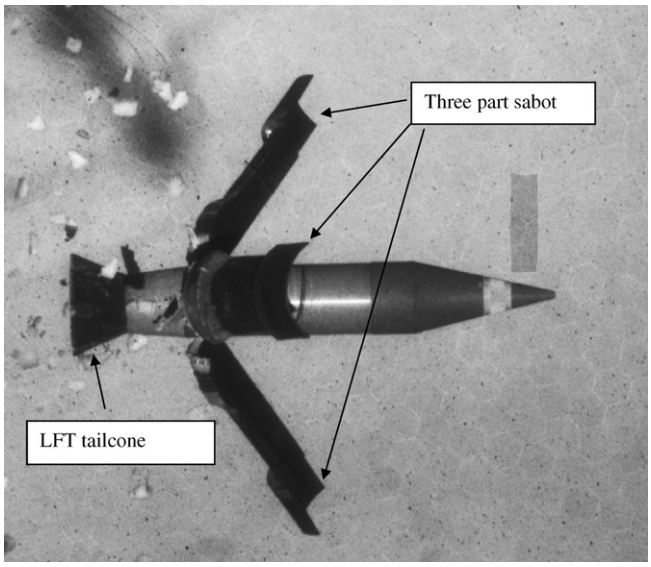

Fig. 22. Fired projectile with filled-back LFT tailcone geometry 5 m away from the barrel. The filled-back tailcone maintained its integrity at a 5 m distance. Note three part discarding sabot.

etry are shown in Fig. 21. The maximum value of the Tsai–Wu failure criterion is found to be 2.185. The area in which failure is presumed to occur corresponds to 1.5% of the total area of the tailcone. In the transition stage, the local failure regions do not compromise the entire geometry, but are limited to two isolated areas, i.e. the bottom left corner (at the first thread) and the top right corner, where the LFT meets the steel projectile. In this case, only 1 of the 26 threads (4%) is seen to fail.

4.5.4. Field testing for the filled-back LFT tailcones

The field testing of the filled-back 40% W_f glass/nylon content LFT tailcones was also conducted at APG, Maryland. The results obtained from these tests for a distance of 5 and 15 m from the exit of the bore obtained with high speed photography are shown in Figs. 22 and 23. The LFT back filled projectiles were successful in reaching the target and surviving the firing conditions.

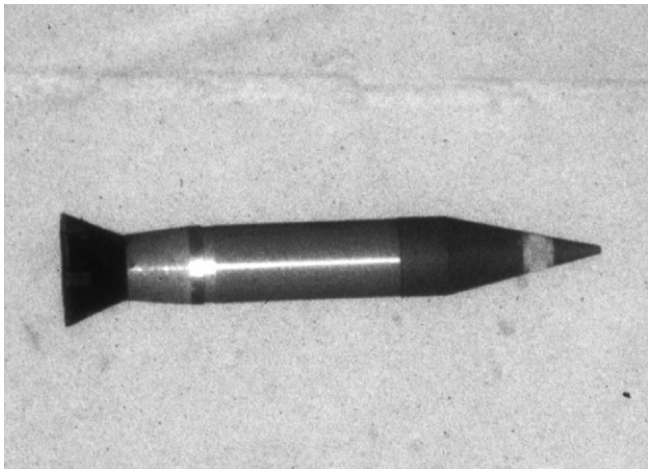

Fig. 23. Fired projectile with filled-back LFT tailcone geometry 15 m away from the barrel. The filled-back tailcone maintained its integrity at a 15 m distance and eventually reached the target.

5. Summary and conclusions

A successful full-cycle design, analysis, tooling, prototype, manufacture and validation of a 40% W_f long fiber thermoplastic (LFT) glass/nylon tailcone for a training round was accomplished.

Among two designs considered, the hollow-back and the filled-back LFT glass/nylon tailcone, the latter was successful in meeting all the loading conditions – including temperature, pressure and gravity loads encountered in the in-bore, transition and out-of-bore stages of the tailcone (attached to the projectile) in field tests. Although the maximum operating temperature of metals (aluminum) is higher than that of polymers (nylon), the thermal conductivity is much lower for the latter. This makes the LFT composite tailcone less prone to failure from temperature for the transient nature of the entire event (in-bore to final flight).

The threaded metal insert was effective in providing integrity to the body of the LFT tailcone at all stages of firing. The threads provided mechanical interlock where local stresses exceeded the yield stress of the material in few of the threads, but did not compromise the body of the tailcone. The successful firing trials were obtained without any pre-treatment of the inserts. Additionally, finite element may be used as a means to re-engineer the component including threads to reduce loads further based on our successful launches and could therefore show the continued value of modeling to reduce net costs for military to validate new materials in munitions applications.

Acknowledgments

The authors acknowledge funding and support for this project provided by the Army Research Laboratory (ARL) under Contract No. W911NF-04-2-0018. The guidance and expertise of Peter Dehmer of ARL is also gratefully acknowledged.

References

[1] <http://www.atk.com/ProductsSolutions/conventionalammo_large-caliber.asp> [accessed March 2005].
[2] Jones A, editor. Reloading manual. Speer; 2001.
[3] Garner J, Bundy M, Newill J. Development of a plastic stabilizer for the M865 training projectile (Technical Report). Army Research Laboratory; 1999.
[4] Hartness T, Husman G, Koenig J, Dyksterhouse J. The characterization of low cost fiber reinforced thermoplastic composites produces by the DRIFT process. Compos Part A 2001;32:1155–60.

[5] Bush SF, Torres FG, Methven JM. Rheological characterization of discrete long glass fibre (LGF) reinforced thermoplastics. Composites 2000;31:1421–31.
[6] <http://www.rtpcompany.com/info/data/index.htm> [accessed January 2005].
[7] Mechanical properties of nylon 6 reinforced with 40% e-glass fiber. <http://www.matweb.com/search/SpecificMaterial.asp?bassnum=O2414> [last accessed July 2006].
[8] Shigley JE, Mischke CR. Mechanical engineering design. 6th ed. New York: McGraw Hill; 2001.
[9] Kohnke P. ANSYS theory reference. Canonsburg, PA: SAS IP, Inc.; 1994.
[10] Chawla KK. Composite materials: science and engineering. 2nd ed. New York: Springer; 2001.
[11] Tsai SW, Hahn HT. Introduction to composite materials. 1st ed. Lancaster: CRC Press; 1980.